University of Banja Luka I Faculty of Architecture, Civil Engineering and Geodesy
ISSN 2712-0570 I UDC 72

2023_11(1)

AGG+ Journal for Architecture, Civil Engineering, Geodesy and Related Scientific Fields
АГГ+ часопис за архитектуру, грађевинарство, геодезију и сродне научне области

046-062 **Categorisation** I Original scientific paper
DOI I 10.61892/AGG20230146
UDC I 66.017:691.2/.4
Paper received I 04/03/2023
Paper accepted I 04/06/2023

Dragan D. Milašinović
University of Novi Sad, Faculty of Civil Engineering Subotica, Serbia,
ddmilasinovic@gmail.com

MATERIAL MEMORY PROPERTIES

Original scientific paper
DOI 10.61892/AGG20230146
UDC 66.017:691.2/.4
Paper received I 04/03/2023
Paper accepted I 04/06/2023

Dragan D. Milašinović
University of Novi Sad, Faculty of Civil Engineering Subotica, Serbia, ddmilasinovic@gmail.com

MATERIAL MEMORY PROPERTIES

ABSTRACT

The study demonstrates that the representative volume of standard cylindrical samples of rocks, concrete and asphalt represents a continuum from which samples are extracted or structures will be built. The rheological-dynamical analogy (RDA) is used as evidence, along with standard experimental data from the samples and the velocities of P and S waves obtained through ultrasonic testing. Unlike all previously existing theories of multiphase materials, the RDA theory uniformly describes the solid state and fluid flow within the representative volume. The solid state and fluid flow are functionally connected by rheological parameters. Plastic viscosity coefficients describe (memorize) the matter in fluid flow at the moment of its natural formation or artificial preparation.

Keywords: *rheological-dynamical analogy, representative volume, solid state, fluid flow, material memory properties*

1. INTRODUCTION

Under the influence of external forces, all bodies undergo more or less deformation, meaning they change their shape and volume. From this, it follows that the entire volume of a body is not filled with matter but is composed of separate small parts (molecules, atoms, elementary particles) that are interconnected by attractive forces. During deformation, the relative positions of particles change, and the internal forces that tend to establish the original arrangement of the particles also change. Therefore, every body represents a discrete medium. To obtain data on the behavior of a body under loading (i.e., to determine the mechanical properties of materials), it is theoretically most appropriate to begin with the existing material structure and base the analysis on data from theoretical physics. However, due to various fundamental difficulties, significant progress in this direction has not been achieved to date.

Instead of the concept of discrete matter structure, it is considered that bodies represent a continuous medium (continuum), leading to the continuum mechanics or the mechanics of continuum. According to this concept, internal forces can be defined as surface forces across imaginary cross-sections within the body. This approach replaces the behavior of a multitude of molecules with certain average values, adopting specific statistical regularities. Deformation of a body is described as a continuous transformation of the space in which the body is situated, which can be considered affine around each point. In this way, the geometry of deformation and the geometry of stress are uniformly determined regardless of the structure and physical properties of the body undergoing deformation. However, to solve the posed problem, it is necessary to establish relationships between stress and the quantities that describe deformation in the vicinity of an arbitrary point within the body. It is known from experience that these relationships depend on certain properties of the observed body, which we precisely call the mechanical properties of materials. The science that deals with this is called rheology.

2. RHEOLOGICAL-DYNAMICAL MODEL OF A CONTINUUM

The rheological behavior of materials is described by relationships between stress and strain and their time derivatives. In this way, the differential equation of the viscoelastoplastic (VEP) material model [1, 2] is formulated.

$$\frac{d^2\varepsilon}{dt^2}+\frac{d\varepsilon}{dt}\left(\frac{E_K}{\lambda_K}+\frac{H'}{\lambda_N}\right)+\varepsilon\frac{E_K H'}{\lambda_K\lambda_N}=\frac{d^2\sigma}{dt^2}\frac{1}{E_H}+\frac{d\sigma}{dt}\left(\frac{E_K}{\lambda_K E_H}+\frac{H'}{\lambda_N E_H}+\frac{1}{\lambda_K}+\frac{1}{\lambda_N}\right)+$$
$$\sigma\left(\frac{E_K}{\lambda_K\lambda_N}+\frac{H'}{\lambda_K\lambda_N}+\frac{E_K H'}{\lambda_K\lambda_N E_H}\right)-\sigma_Y\frac{E_K}{\lambda_K\lambda_N} \quad . \qquad (1)$$

In a fixed time interval, there are five rheological constants of the material: the elasticity modulus E_H, the viscoelastic (VE) modulus E_K, longitudinal VE viscosity λ_K, the slope of linear hardening H', and longitudinal viscoplastic (VP) viscosity λ_N. These constants cannot be easily determined through physical experiments, especially the coefficients of longitudinal Trouton viscosity. Primarily due to this, it was necessary to seek an alternative approach to address this complex problem.

Let us analyze the homogeneous equation from equation (1), multiplied by the product of longitudinal viscosities $\lambda_K \lambda_N$,

$$\frac{d^2\varepsilon}{dt^2}\lambda_K\lambda_N + \frac{d\varepsilon}{dt}\left(E_K\lambda_N + H'\lambda_K\right) + \varepsilon E_K H' = 0 \quad . \tag{2}$$

It is apparent that equation (2) is a mathematical analogue to the differential equation of damped vibrations. However, the important question is the following dimensional analysis as well. In mechanics, there are three fundamental measurement quantities: mass (*M*), length (*L*), and time (*T*). All others can be derived from them. Thus we have

$$\left[\lambda_K\right],\left[\lambda_N\right] = ML^{-1}T^{-1}, \left[E_K\right],\left[H'\right] = ML^{-1}T^{-2}, \left[\rho\right] = ML^{-3}, \left[g\right] = LT^{-2},$$

$$\left[\gamma\right] = \left[\rho g\right] = ML^{-2}T^{-2},$$

$$\left[\lambda_K\lambda_N\right] = M^2L^{-2}T^{-2} = M\left[\gamma\right] = \left[m\gamma\right],$$

$$\left[E_K\lambda_N + H'\lambda_K\right] = M^2L^{-2}T^{-3} = MT^{-1}\left[\gamma\right] = \left[c\gamma\right],$$

$$\left[E_K H'\right] = M^2L^{-2}T^{-4} = MT^{-2}\left[\gamma\right] = \left[k\gamma\right]. \tag{3}$$

Clearly, we can also talk about the physical analogy between the rheological equation (2) and the equation of damped vibrations. If we divide the rheological constants in equation (2) by the material volumetric weight γ , we obtain physical notions: mass, damping, and stiffness.

$$m = \frac{\lambda_K\lambda_N}{\gamma}\left[\frac{N\cdot s^2}{m}\right],\ c = \frac{E_K\lambda_N + H'\lambda_K}{\gamma}\left[\frac{N\cdot \mathrm{s}}{m}\right],\ k = \frac{E_K H'}{\gamma}\left[\frac{N}{m}\right]. \tag{4}$$

Equation (2) now takes the following form

$$\frac{d^2\varepsilon}{dt^2}m + \frac{d\varepsilon}{dt}c + \varepsilon k = 0\,. \tag{5}$$

The occurrence of this mathematical-physical analogy is not accidental. It arises from Hooke's law, which was originally formulated in two ways, with two expressions: 1) and 2), as shown in Figure 1 [3]. The first expression relates displacement and loading, as shown in Figure 1 a). The second expression relates stress and strain, as shown in Figure 1 b). Both expressions involve the elasticity modulus E_H as a material constant.

$$u = \frac{Ql_0}{A_0 E_H} \qquad 1)$$

$$\sigma = E_H \varepsilon \qquad 2)$$

$$\Rightarrow E_H \equiv \frac{Ql_0}{A_0 u} = \frac{\sigma}{\varepsilon}$$

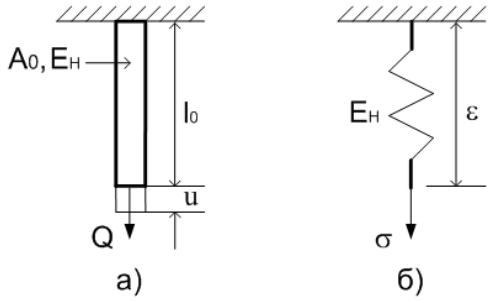

Figure 1. Hooke's law: a) Loading – displacement, b) Stress – strain

Although the second way of writing Hooke's law is the actual basis for deriving rheological equations, the first way, from a historical perspective, was not without significance. It served as a prototype for the theory of elasticity through the definition of superposition principles, Maxwell's reciprocal relations, Betti-Rayleigh reciprocal theorems, deformation energy, Castigliano's theorem, the principle of virtual work, etc. It also becomes important when applying RDA [1], as shown in Figure 2.

$$\sigma_{SV} = Y = \sigma_Y + H'\varepsilon_{vp}$$

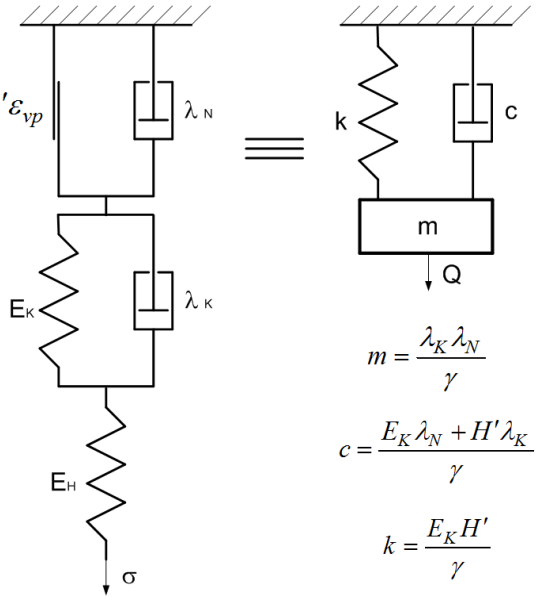

$$m = \frac{\lambda_K \lambda_N}{\gamma}$$

$$c = \frac{E_K \lambda_N + H' \lambda_K}{\gamma}$$

$$k = \frac{E_K H'}{\gamma}$$

Figure 2. The analogy between the VEP rheological model and the damped dynamic model.

Let us consider a dry sample or the representative volume V on the left side of Figure 3, which includes the volume of pores V_p and the volume of solid matter without pores V_0.

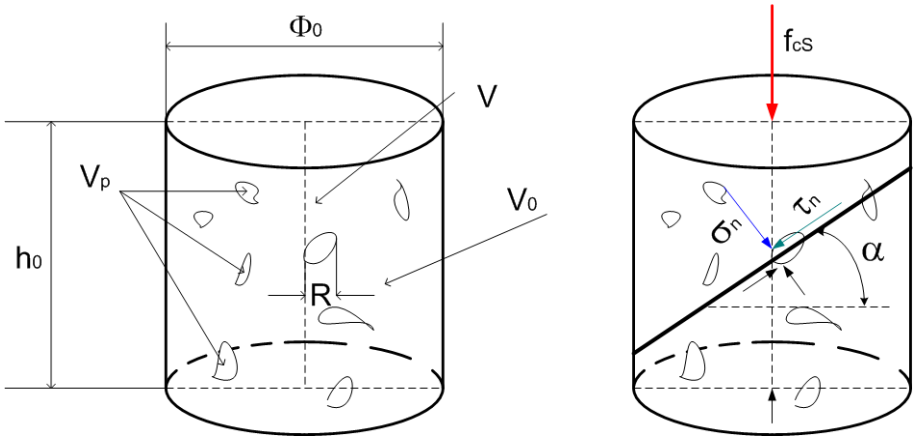

Figure 3. Sample or representative volume on the left with an imaginary fracture plane on the right.

Porosity is defined by the equation

$$p = \frac{V_p}{V} = \frac{V - V_0}{V} = 1 - \frac{V_0}{V}. \tag{6}$$

Calculating the volume of pores is a challenging problem, but it (6) can be expressed in the following way

$$p = 1 - \frac{m_0/\rho_0}{m/\rho}. \tag{7}$$

In a dry sample $m_0 \approx m$, because the mass of air in the pores is negligible, thus leading to

$$p = 1 - \frac{\rho}{\rho_0}. \tag{8}$$

In samples under load, both pores and cracks are present, so we refer to the void volume fraction (VVF), whose definition remains unchanged compared to the definition of porosity

$$VVF = 1 - \frac{\rho}{\rho_0}. \tag{9}$$

Porosity or VVF has been extensively studied in all materials for a very long time, and one of the first relations describing the influence of porosity on the elastic modulus E_H was linear

$$E_H(p) = E_{H,0}(1 - p), \tag{10}$$

where the material's elastic modulus $E_{H,0}$ is with zero porosity.

Let us take as an example a sandstone sample with a height h_0 =0.1418 and a diameter Φ_0 =0.0735 m [4]. The stiffness and mass of the sample are

$k = E_H(p) A_0 / h_0 = 41831 \cdot 10^6 \cdot 0.0735^2 \cdot \pi / 4 / 0.1418 = 1251660582$ N/m,

$m = \rho V_0 = 2526 \cdot 0.1418 \cdot 0.0735^2 \cdot \pi / 4 = 1.52$ kg.

The dynamic delay time and propagation time of the P-wave are

$T^D = \sqrt{m/k} = 0.000034845$ s,

$T_L^D = T^D \sqrt{\Psi} = 0.000034845 \cdot \sqrt{0.81} = 0.0000314$ s.

Time T_L^D appears on the display of the ultrasound machine (Time 1) as the first signal and corresponds to the speed of the longitudinal wave, which has the highest velocity and is called the P-wave. Another signal (Time 2) appears on the display, corresponding to the speed of the transverse S-wave. Based on these two times and the dimensions of the sample, the velocities of the P and S waves are calculated. The calculated velocity of the P-wave (4522 m/s) is indicated on the apparatus display as (Velocity), while the velocity of the S-wave (2559 m/s) is marked as (Velocity 2).

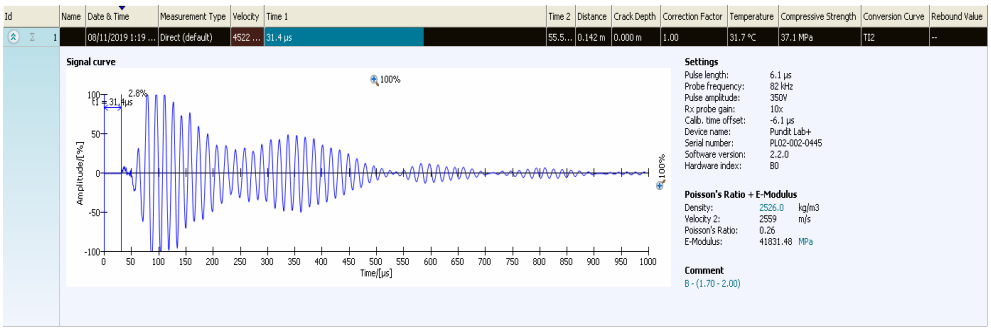

Figure 4. Display of the ultrasound testing device "PUNDIT LAB - 4x1.5V AA (LR6): PL0V-002-0445".

The dynamic modulus of elasticity and the shear modulus are, respectively:

$E_D = 4522^2 \cdot 2526 = 51652.87$ MPa,

$G_H = 2559^2 \cdot 2526 = 16541.46$ MPa.

Poisson's ratio, creep coefficient, and modulus of elasticity are, respectively [5]:

$$\mu = \frac{4522^2 - 2 \cdot 2559^2}{2\left(4522^2 - 2559^2\right)} = 0.26444,$$

$$\varphi = \frac{2 \cdot 0.26444}{1 - 2 \cdot 0.26444} = 1.12263,$$

$E_H = 2(1 + 0.26444) \cdot 16541.46 = 41831.48$ MPa.

The obtained Poisson's coefficient and modulus of elasticity correspond to the parameters displayed on the device, as shown in Figure 4. The modulus of elasticity ratio falls within the limits experimentally confirmed for brittle materials such as concrete and rocks.

$$\Psi = \frac{41831.48}{51652.87} = 0.81 .$$

The rheological properties of the sandstone sample in a state of critical damping are:

$E_{K,cr} = E_H(p)/\varphi = 41831 \cdot 10^6 / 1.12263 = 37261658909$ N /m^2,

$\lambda_{K,cr} = E_{K,cr} T^D = 37261658909 \cdot 0.000034845 = 1298398$ Ns /m^2,

$\eta_{K,cr} = \lambda_{K,cr}/3 = 432799$ Pas,

$H'_{cr} = k\gamma / E_{K,cr} = 1251660582 \cdot 2526 \cdot 10 / 37261658909 = 848.52$ N /m^2,

$\lambda_{N,cr} = H'_{cr} T^D = 848.52 \cdot 0.000034845 = 0.029567$ Ns /m^2,

$\eta_{N,cr} = \lambda_{N,cr}/3 = 0.01$ Pas,

$m = \lambda_{K,cr}\lambda_{N,cr}/\gamma = 1298398 \cdot 0.029567 / 2526 \cdot 10 = 1.52$ kg.

The coefficient of shear viscosity $\eta_{K.cr}$ corresponds to the VE polymer, while $\eta_{N,cr}$ corresponds to the viscosity of oil; it is clear that the RDA model includes the properties of fluids in the solid sample or the representative volume.

When it comes to volume, the fundamental question is to determine its continuum character in order to ensure the validity of the calculated mechanical characteristics. On the display in Figure 4, the frequency of the ultrasonic probe is stated as f_σ = 82 kHz, as well as a pulse length of 6.1 μs. Since the period $T_\sigma = 1/f_\sigma$ = 12.2 μs (also $T_\sigma = 2 \cdot 6.1$ μs), the ultrasonic device has achieved a wavelength of $\lambda = v_L T_\sigma = 4522 \cdot 0.0000122 = 0.055$ m. On the other hand, we must also introduce pores or capillaries into the analysis, whose diameter can be within the range of $2 \cdot 10^{-7} \langle R \langle 2 \cdot 10^{-3}$ m. This is a physical condition because, for diameters smaller than $2 \cdot 10^{-7}$ m, moisture does not transport through the capillary, while for diameters larger than $2 \cdot 10^{-3}$ m, attractive molecular forces are not sufficient to enable capillary transport. Taking into account the upper limit of 0.002 m, the wavelength is 27.5 times larger than the pore diameter (0.055/0.002 = 27.5), while for the lower limit, it is 275,000 times larger. The wavelengths achieved by the ultrasonic devices are much larger than the pore diameter, thus ensuring that the representative volume (sample) is a continuum that is uniquely described by the solid matter with inclusions and fluid in the flow phase. This is a fundamental contribution to the RDA theory of continuum mechanics. Theorem I states:

I. If the rheological time delay of VE deformation T_K is equal to the time delay of VP deformation T^*, then the times are equal to the dynamic time delay T^D during the propagation of an elastic wave in a bar, as shown in Figure 1a), which is in a state of critical damping.

Proof:

From the dynamic model, we have

$$c_{cr} = 2\sqrt{km} = 2A_0\sqrt{E_H \rho} .$$

From the rheological model, we have

$$c_{cr} = 2\sqrt{k\frac{\lambda_K \lambda_N}{\gamma}} = 2\sqrt{k\frac{E_K H'}{\gamma}\frac{\lambda_K \lambda_N}{E_K H'}} = 2\sqrt{k^2 T_K T^*} = 2\sqrt{k^2 T^{D2}} = 2kT^D .$$

Thus, the analogy gives

$$2A_0\sqrt{E_H \rho} = 2kT^D \qquad \Rightarrow \qquad T^D = \frac{l_0\sqrt{E_H \rho}}{E_H} = l_0\sqrt{\frac{\rho}{E_H}} = \frac{l_0}{v_0} .$$

3. MATERIAL MEMORY PROPERTIES

From a continuum perspective, there are many material properties associated with memory, so it is rightfully considered impossible to establish a single definition of material memory. However, if we consider rheological properties according to the RDA theory, the memory characteristics of materials can be explained by the coefficients of shear viscosity, whose unit of measurement involves stress and time. It has already been demonstrated on a sandstone sample that the shear viscosity coefficient $\eta_{K,cr}$ corresponds to VE polymers and $\eta_{N,cr}$ to the viscosity of oil, thereby proving that the RDA model of solid matter incorporates both the characteristics of a fluid in a representative volume. Starting from the fundamental equations (4), where

$$\omega = \sqrt{\frac{k}{m}} = \frac{1}{\sqrt{T_K T^*}}, \tag{11}$$

we define critical damping

$$c_{cr} = 2\sqrt{km} = 2k\sqrt{T_K T^*} . \tag{12}$$

Furthermore, it follows that damping is

$$c = \frac{E_K H' T^* + H' E_K T_K}{\gamma} = k\left(T_K + T^*\right). \tag{13}$$

So, the coefficient of viscous damping is

$$\xi = \frac{c}{c_{cr}} = \frac{T_K + T^*}{2\sqrt{T_K T^*}} . \tag{14}$$

However, according to the RDA theory, the sample can also be in a state of overdamping, exceeding the critical level. This occurs in the case of damping defined as follows: [5]

$$\xi = \frac{\xi_{cr}}{1 - D_1} = \frac{1}{1 - 2\mu_D}, \tag{15}$$

where D_1 is the scalar variable of damage. In the case of critical damping, the following also holds true

$$c_{cr} = 2kT^D = 2\frac{E_H(p)A_0}{l_0}l_0\sqrt{\frac{\rho}{E_H(p)}} = 2A_0\sqrt{E_H(p)\rho}\,, \tag{16}$$

so damping greater than critical damping is defined by measured mechanical properties of the material and the geometry of the sample as follows:

$$c = \xi c_{cr} = \frac{1}{1-2\mu_D}2A_0\sqrt{E_H(p)\rho}\,. \tag{17}$$

In this way, all three parameters of the dynamic model m, c and k are defined. However, the system of three equations (4) is indeterminate because it involves four parameters of the rheological model E_K, H', λ_K and λ_N. The elastic longitudinal wave propagates in the solid material with a phase velocity v_0, so according to [5], the VE modulus is

$$E_K = \frac{E_H(p)}{\varphi_c} = \frac{E_H(p)(1-2\mu_D)}{2\mu_D}\,. \tag{18}$$

Using the third equation (4), we define the slope of linear amplification

$$H' = k\frac{2\mu_D}{E_H(p)(1-2\mu_D)}\gamma = \frac{A_0}{l_0}\frac{2\mu_D}{1-2\mu_D}\gamma\,. \tag{19}$$

By substituting expressions (18) and (19) into the second equation (4), we obtain a quadratic equation

$$A\lambda_K^2 + B\lambda_K + C = 0\,, \tag{20}$$

where:

$$A = 2\mu_D H'\,,\ B = -2c\mu_D\gamma\,,\ C = E_H(p)(1-2\mu_D)m\gamma\,. \tag{21}$$

The roots of the quadratic equation (20) yield the VE coefficients of longitudinal viscosity in a state of deformation greater than the critical

$$\lambda_{K,1/2} = \frac{-B \pm \sqrt{B^2 - 4AC}}{2A}\,. \tag{22}$$

The first equation (4) yields the VP coefficients of longitudinal viscosity

$$\lambda_{N,1/2} = \frac{m\gamma}{\lambda_{K,1/2}}\,. \tag{23}$$

The shear viscosities are equal to one-third of the longitudinal ones. For the analyzed sample of sandstone, we obtain:

$$c = \frac{1}{1-2\cdot 0.26443} 2\cdot 0.00424917\sqrt{41831\cdot 10^6\cdot 2526} = 185155 \text{ Ns/m}, \quad \xi = \frac{185155}{87229} = 2.12,$$

$\lambda_{K,cr} = 1298398$ Pas, $\lambda_{K1} = 5187023$ Pas, $\lambda_{K2} = 325011$ Pas,

$\lambda_{N,cr} = 0.03$ Pas, $\lambda_{N1} = 0.007$ Pas, $\lambda_{N2} = 0.118$ Pas,

$\eta_{N,cr} = 0.01$ Pas, $\eta_{N1} = 0.002$ Pas, $\eta_{N2} = 0.039$ Pas.

The calculated shear viscosities correspond to fluids that are between water and oil.

3.1. SAMPLES OF GRANITE ROCK FROM LAC DU BONNET, CANADA

In the works [6] and [4], the mechanical behavior of Lac du Bonnet granite was simulated. Four PFC2D and four PFC3D granite materials were produced. The test results of macro properties are presented in Tables 1 and 2 in terms of the mean values of each macro property [6].

Table 1. Macro Properties of PFC2D Lac du Bonnet Granite: Diameter of 63mm (Slenderness 2.5).

Material	PFC2D-1	PFC2D-2	PFC2D-3	PFC2D-4
ρ [kg /m³]	2630	2630	2630	2630
$E_H(p)$ [MPa]	68300	68800	70900	71500
f_{cS} [MPa]	186.8	184.4	199.1	194.8
μ_D	0.231	0.249	0.237	0.245
φ_c	0.858736	0.992032	0.901141	0.960784
$E_{K,cr}$ [MPa]	79535.50	69352.61	78678.06	74418.37
m [kg]	1.291	1.291	1.291	1.291
c_{cr} [Ns/m]	83558.22	83863.52	85133.79	85493.26
k [N/m]	1351795903	1361691920	1403255191	1415130411
ξ	1.858736	1.992032	1.901141	1.960784
c [Ns/m]	155312.68	167058.80	161851.31	167633.84
H' [Pa]	447.00	516.38	469.07	500.12
A	206.51	257.16	222.34	245.06
B	-1887142304	-2188035900	-2017670823	-2160297303
C	1.24786E+15	1.17288E+15	1.26647E+15	1.23834E+15
λ_{K1} [Pas]	8420524.52	7933618.57	8396314.08	8199153.87
λ_{K2} [Pas]	717594.37	574887.33	678405.3	616314.04
λ_{N1} [Pas]	0.00403	0.00428	0.00404	0.00414
η_{N1} [Pas]	**0.00134**	**0.00143**	**0.00135**	**0.00138**
λ_{N2} [Pas]	0.04732	0.05907	0.05006	0.0551
η_{N2} [Pas]	**0.01577**	**0.01969**	**0.01669**	**0.01837**
$\lambda_{K,cr}$ [Pas]	2458153.98	2135634.98	2386651.2	2247944.32
$\lambda_{N,cr}$ [Pas]	0.0138	0.0159	0.0142	0.0151
$\eta_{N,cr}$ [Pas]	**0.0046**	**0.0053**	**0.0047**	**0.005**

Table 2. Macro Properties of PFC3D Lac du Bonnet Granite: Diameter of 63 mm (Slenderness 2.5).

Material	PFC3D-1	PFC3D-2	PFC3D-3	PFC3D-4
ρ [kg /m³]	2630	2630	2630	2630
$E_H(p)$ [MPa]	57300	64000	67600	69200
f_{cS} [MPa]	127.9	169.6	186.9	198.8
μ_D	0.231	0.254	0.255	0.256
φ_c	0.858736	1.032520	1.040816	1.049180
$E_{K,cr}$ [MPa]	66725.97	61984.25	64949.02	65956.25
m [kg]	1.291	1.291	1.291	1.291
c_{cr} [Ns/m]	76534.31	80885.16	83128.93	84106.95
k [N/m]	1134083532	1266690158	1337941479	1369608733
ξ	1.858736	2.032520	2.040816	2.049180
c [Ns/m]	142257.08	164400.73	169650.88	172350.31
H' [Pa]	447.00	537.46	541.78	546.13
A	206.51	273.03	276.31	279.62
B	-1728508858	-2196459477	-2275527261	-2320800369
C	1.04689E+15	1.06932E+15	1.12488E+15	1.1468E+15
λ_{K1} [Pas]	7712694.05	7524272.62	7707313.95	7772183.34
λ_{K2} [Pas]	657273.29	520517.21	528216.93	527690.95
λ_{N1} [Pas]	0.00440	0.00451	0.00441	0.00437
η_{N1} [Pas]	**0.00147**	**0.0015**	**0.00147**	**0.00146**
λ_{N2} [Pas]	0.05167	0.06524	0.06429	0.06436
η_{N2} [Pas]	**0.01722**	**0.02175**	**0.02143**	**0.02145**
$\lambda_{K,cr}$ [Pas]	2251521.22	1979018.30	2017705.07	2025169.33
$\lambda_{N,cr}$ [Pas]	0.0151	0.0172	0.0168	0.0168
$\eta_{N,cr}$ [Pas]	**0.005**	**0.0057**	**0.0056**	**0.0056**

The critical shear viscosities calculated using the RDA theory range from **0.0046** to **0.0057** Pas. The highest measured viscosity of the liquid metal, **0.0065** Pas, is found in uranium [7]. However, these results can be correlated with the findings in [8], which reported elevated concentrations of uranium in groundwater samples collected from supply wells and exploration boreholes in the vicinity of the underground research laboratory in the southeastern region of Manitoba, Canada. All groundwater originates from the Lac du Bonnet granite basin or the sediments covering the basin.

3.2. SAMPLES OF GRANITE ROCK FROM THE HENGYANG REGION, CHINA

In the works [9], [10], and [4], the behavior of granite from the Hengyang region, China, was simulated. In this study, four granite samples labeled as F1 were analyzed. The test results of macro properties are presented in Table 3.

Table 3. Macro Properties of Granite Rock from the Hengyang Region: Diameter of 50 mm (Slenderness 2)

Material	F1-24	F1-6	F1-7	F1-15
ρ [kg /m^3]	2710	2710	2710	2710
$E_H(p)$ [MPa]	49043	46700	52500	50500
f_{cS} [MPa]	143.43			
μ_D	0.235263	0.235	0.235	0.235
φ_c	0.88867	0.88679	0.88679	0.88679
$E_{K,cr}$ [MPa]	55187.16	52661.70	59202.13	56946.81
m [kg]	0.532	0.532	0.532	0.532
c_{cr} [Ns/m]	45272.35	44177.69	46840.79	45939.92
k [N/m]	962957053.2	916952355.8	1030835089	991565181.3
ξ	1.88867	1.88679	1.88679	1.88679
c [Ns/m]	85504.39	83354.13	88378.84	86679.09
H' [Pa]	472.87	471.87	471.87	471.87
A	222.5	221.78	221.78	221.78
B	-1090288230	-1061681502	-1125681327	-1104031588
C	3.74447E+14	3.56912E+14	4.01239E+14	3.85954E+14
λ_{K1} [Pas]	4528643.62	4423302.5	4689946.1	4599746.41
λ_{K2} [Pas]	371620.96	363827.53	385759.62	378340.47
λ_{N1} [Pas]	0.00318	0.00326	0.00307	0.00313
η_{N1} [Pas]	**0.0011**	**0.0011**	**0.001**	**0.001**
λ_{N2} [Pas]	0.0388	0.03963	0.03738	0.03811
η_{N2} [Pas]	**0.0129**	**0.0132**	**0.0125**	**0.0127**
$\lambda_{K,cr}$ [Pas]	1297281.34	1268589.46	1345062.02	1319193.02
$\lambda_{N,cr}$ [Pas]	0.0111	0.0114	0.0107	0.0109
$\eta_{N,cr}$ [Pas]	**0.0037**	**0.0038**	**0.0036**	**0.0036**

The critical shear viscosities calculated using the RDA theory range from **0.0036** to **0.0038** Pas. These viscosities can be associated with the viscosities found in pure gold at its melting point, ranging from **0.00358** to **0.00484** Pas [7]. However, according to reports in [11], the Hunan province to which the Hengyang city region belongs is rich in gold. Extremely high-quality Au mineralization is developed in quartz-sulfide veins controlled by faults. The sulfide/sulfosalts complex is dominated by pyrite, chalcopyrite, and galena, with minor tetrahedrite and chalcocite. Alteration includes beresitization and carbonization. Based on the cross-cutting relationships of veins and mineral assemblages, the hydrothermal period consists of three phases: (1) quartz-pyrite pre-ore, (2) syn-ore quartz-ankerite-native gold-sulfide-sulfosalts, and (3) post-ore quartz-calcite-pyrite alteration. Au native gold predominates in appearance, with minor Au native gold nanoparticles (within sulfides).

3.3. SAMPLES OF RECYCLED AGGREGATE CONCRETE, GERMANY

Let us further examine experimental data for various concrete mixes made from recycled aggregate [12]. One mix of standard concrete and four concrete mixes with recycled aggregate were analyzed. The recycled aggregates were generated from two different

types of recycled bricks (ZB1 and ZB2) and recycled calcium silicate bricks (BZK) with particle sizes of 2-8 mm and 8-16 mm. For the particle size fraction of 0-2 mm, sand from the River Rheine was used. The test results of macro properties are presented in Table 4.

Table 4. Experimentally Estimated Mechanical Properties of Standard Concrete and Concrete with Four Mixes of Recycled Aggregate (Müller [12]). Cylindrical samples: diameter of 150 mm (Slenderness 2)

Material	ZB1	BZK1	BZK2	ZB2	Standard concrete
ρ [kg /m³]	2060	2120	2160	1950	2442.85
$E_H(p)$ [MPa]	16300	19700	20600	16000	34510
f_{cS} [MPa]	31.8	28.6	29.2	21	48.63
μ_D	0.18455	0.16025	0.15255	0.17793	0.25196
φ_c	0.58504	0.47167	0.43906	0.55246	1.01580
$E_{K,cr}$ [MPa]	27861.47	41766.46	46918.85	28961.50	33973.1
m [kg]	10.921	11.239	11.451	10.338	12.821
c_{cr} [Ns/m]	204799.93	228403.86	235756.07	197414.79	324506.41
k [N/m]	960149254.8	1160425786	1213440162	942477796.1	2053340198
ξ	1.58504	1.47167	1.43906	1.55246	2.01580
c [Ns/m]	324615.52	336135.19	339266.18	306478.08	654141.28
H' [Pa]	709.91	589.01	558.63	634.58	1476.46
A	262.03	188.78	170.44	225.82	744.02
B	-2468201124	-2283904143	-2235818411	-2126734170	-8052485520
C	2.31354E+15	3.18949E+15	3.54071E+15	2.07761E+15	5.36191E+15
λ_{K1} [Pas]	8364006.54	10487261.04	11275668.15	8310771.74	10110135.10
λ_{K2} [Pas]	1055640.24	1611036.47	1842389.30	1107026.30	712816.83
λ_{N1} [Pas]	0.02690	0.02272	0.02194	0.02426	0.030979
η_{N1} [Pas]	**0.009**	**0.0076**	**0.0073**	**0.0081**	**0.01**
λ_{N2} [Pas]	0.21311	0.14790	0.13425	0.18210	0.439384
η_{N2} [Pas]	**0.071**	**0.0493**	**0.0448**	**0.0607**	**0.1465**
$\lambda_{K,cr}$ [Pas]	2971427.58	4110396.58	4557869.06	3033190.22	2684525.00
$\lambda_{N,cr}$ [Pas]	0.0757	0.0580	0.0543	0.0665	0.1167
$\eta_{N,cr}$ [Pas]	**0.0252**	**0.0193**	**0.0181**	**0.0222**	**0.0389**

According to the study [13], the plastic viscosity of cementitious materials depends on a wide range of factors. At a temperature of $23^{\circ}C$, the viscosity measured with a rheometer was **0.07** Pas, whereas at $60^{\circ}C$, it was **0.03** Pas [13]. Clearly, the calculated plastic viscosities in Table 4 fall within the range of the measured values. Standard concrete is closer to the measured viscosities. The RDA theory also showed that recycled concretes with brick aggregate have lower values of plastic viscosity. Once again, the RDA theory observes minor differences in concrete mixes, as demonstrated in the case of rotational capacities in reference [14].

3.4. ASPHALT SAMPLES WITH BGA ADDITIVES, INDONESIA

The compressive strength of asphalt concrete binder (AC-BC) mixed with granular asphalt (BGA) from Indonesia was tested in the study [15]. The results of the testing of macro properties are presented in Table 5.

Table 5. Macro properties of asphalt samples AS-BC: diameter of 101.6 mm and length of 63.5 mm.

Material	AC-BC without BGA	AC-BC with 5% BGA	AC-BC with 8% BGA
ρ [kg /m^3]	2550	2550	2550
$E_H(p)$ [MPa]	327.95	410.82	415
f_{cS} [MPa]	3.53	4.45	3.88
μ_D	0.37	0.33	0.31
φ_c	2.84615	1.94118	1.63158
$E_{K,cr}$ [MPa]	115.23	211.63	254.35
m [kg]	1.313	1.313	1.313
c_{cr} [Ns/m]	14827.95	16595.99	16680.21
k [N/m]	41870795.03	52451166.38	52984845.06
ξ	3.84615	2.94118	2.63158
c [Ns/m]	57030.59	48811.74	43895.28
H' [Pa]	9266.21	6319.88	5311.92
A	6857.00	4171.12	3293.39
B	-1076167204	-821501519.8	-693984394.7
C	2.85438E+12	4.67586E+12	5.27914E+12
λ_{K1} [Pas]	154245.66	191083.25	202816.77
λ_{K2} [Pas]	2698.77	5866.60	7903.43
λ_{N1} [Pas]	0.21703	0.17519	0.16505
η_{N1} [Pas]	**0.0723**	**0.0584**	**0.055**
λ_{N2} [Pas]	12.40412	5.70617	4.23561
η_{N2} [Pas]	**4.135**	**1.902**	**1.412**
$\lambda_{K,cr}$ [Pas]	20402.78	33481.48	40036.84
$\lambda_{N,cr}$ [Pas]	1.6407	1.0000	0.8361
$\eta_{N,cr}$ [Pas]	**0.5469**	**0.3333**	**0.2787**

In this study, plastic viscosities of asphalt samples with varying percentages of BGA additives were calculated using the RDA theory. It was demonstrated that viscosity decreases with increasing percentages of BGA additives, as expected. The study [16] presented the results of testing the physical properties of asphalt binder. It emphasizes that numerous factors influence the results of plastic viscosities, but it is noted that at a temperature of $135^\circ C$ the viscosity is **0.413** Pas, and it decreases to **0.1** Pas at a temperature of $165^\circ C$. Comparing these values with the critical values of plastic viscosities in Table 5, satisfactory accuracy can be observed for all analyzed asphalts.

4. CONCLUSION

In the concluding remarks, it can be emphasized that material parameters, according to the RDA theory, are defined in two states: critical deformation and deformation greater than critical. Both states relate to the material particle (sample or representative volume V) in either a solid state or fluid flow. When considering the solid state of matter, the moduli E_K and H' are used, while for the fluid flow, the shear viscosities η_K and η_N are used.

The focus of experimental data is on the inelastic deformation of cylindrical dry samples in the solid state, where moduli are crucial for strength, while viscosities describe the VE (Viscous Elastic) and VP (Viscous Plastic) responses of the material, leading to the critical point of strength as shown in Figure 3 on the right and the ultimate deformation.

A key conclusion can be that the calculated shear plastic viscosities for all analyzed materials represent the viscosities of these materials in the phase of their fluid flow, which occurs during their natural formation at high temperatures or during their artificial preparation in laboratory conditions when the materials are fresh before they begin to harden. Therefore, it can be concluded that the plastic viscosities calculated by the RDA theory are a material memory property.

5. REFERENCES

[1] D. D. Milašinović , “Reološko-dinamička analogija,” in *Naučni skup SANU “Mehanika, materijali i konstrukcije,”* 1996, pp. 103–110.

[2] Milašinović D. D., *The Finite Strip Method in Computational Mechanics*. Subotica, Yugoslavia: Faculty of Civil Engineering, 1997.

[3] Y. Fung and P. Tong, *Classical and Computational Solid Mechanics*. World Scientific, 2001.

[4] D. D. Milašinović, “Rheological-dynamical method for prediction of compressive strength and deformation of rocks,” *International Journal of Rock Mechanics and Mining Sciences*, vol. 141, p. 104659, May 2021, doi: https://doi.org/10.1016/j.ijrmms.2021.104659.

[5] D. Milasinovic, “Rheological-dynamical Continuum Damage Model for Concrete under Uniaxial Compression and Its Experimental Verification,” *Theoretical and Applied Mechanics*, vol. 42, no. 2, pp. 73–110, 2015, doi: https://doi.org/10.2298/tam1502073m.

[6] D. O. Potyondy and P. A. Cundall, “A bonded-particle model for rock,” *International Journal of Rock Mechanics and Mining Sciences*, vol. 41, no. 8, pp. 1329–1364, Dec. 2004, doi: https://doi.org/10.1016/j.ijrmms.2004.09.011.

[7] D. Ofte, “The Viscosities of Liquid uranium, Gold and Lead,” *Journal of Nuclear Materials*, vol. 22, no. 1, pp. 28–32, Apr. 1967, doi: https://doi.org/10.1016/0022-3115(67)90105-5.

[8] M. Gascoyne, “High Levels of Uranium and Radium in Groundwaters at Canada’s Underground Research Laboratory, Lac Du Bonnet, Manitoba, Canada,” *Applied Geochemistry*, vol. 4, no. 6, pp. 577–591, Nov. 1989, doi: https://doi.org/10.1016/0883-2927(89)90068-1.

[9] J.-Q. Xiao, D.-X. Ding, F.-L. Jiang, and G. Xu, “Fatigue Damage Variable and Evolution of Rock Subjected to Cyclic Loading,” *International Journal of Rock Mechanics and*

Mining Sciences, vol. 47, no. 3, pp. 461–468, Apr. 2010, doi: https://doi.org/10.1016/j.ijrmms.2009.11.003.
[10] J. Xiao, D. Ding, G. Xu, and F. Jiang, "Inverted S-shaped Model for Nonlinear Fatigue Damage of Rock," *International Journal of Rock Mechanics and Mining Sciences*, vol. 46, no. 3, pp. 643–648, Apr. 2009, doi: https://doi.org/10.1016/j.ijrmms.2008.11.002.
[11] S.-M. Chen *et al.*, "Genesis of Chaxi Gold Deposit in Southwestern Hunan Province, Jiangnan Orogen (South China): Constraints from Fluid Inclusions, H-O-S-Pb Isotopes, and Pyrite Trace Element Concentrations," *Minerals*, vol. 12, no. 7, pp. 867–867, Jul. 2022, doi: https://doi.org/10.3390/min12070867.
[12] C. Müller, Beton als kreislaufgerechter Baustoff DafStb, Heft 513. Berlin: Beuth Verlag, 2001.
[13] A. Shahriar and M. L. Nehdi, "Rheological Properties of Oil Well Cement Slurries," *Proceedings of the Institution of Civil Engineers - Construction Materials*, vol. 165, no. 1, pp. 25–44, Feb. 2012, doi: https://doi.org/10.1680/coma.2012.165.1.25.
[14] D. D. Milašinović, D. Goleš, A. Pančić, and A. Čeh, "Rheological-dynamical Model of Concrete and Its Application on RC Beams," *Mechanics of Time-Dependent Materials*, vol. 26, no. 1, pp. 79–99, Nov. 2020, doi: https://doi.org/10.1007/s11043-020-09476-8.
[15] A. Gaus, M. W. Tjaronge, N. Ali, and R. Djamaluddin, "Compressive Strength of Asphalt Concrete Binder Course (AC-BC) Mixture Using Buton Granular Asphalt (BGA)," *Procedia Engineering*, vol. 125, pp. 657–662, 2015, doi: https://doi.org/10.1016/j.proeng.2015.11.097.
[16] R. Muniandy, E. Aburkaba, and R. Taha, "Effect of Mineral Filler Type and Particle Size on the Engineering Properties of Stone Mastic Asphalt Pavements," *The Journal of Engineering Research [TJER]*, vol. 10, no. 2, p. 13, Dec. 2013, doi: https://doi.org/10.24200/tjer.vol10iss2pp13-32.

Acknowledgements

The present work has been supported by The Provincial Secretariat for Higher Education and Scientific Research, Autonomous Province of Vojvodina, Republic of Serbia (Project No. 142-451-2640/2021-01).

AUTHORS' BIOGRAPHIES

Dragan D. Milašinović

He finished elementary and high school in his hometown of Sarajevo. He graduated from the Faculty of Civil Engineering in Sarajevo in 1978. At this faculty, he defended his master's thesis: "Finite Strip Method in Structural Analysis" in 1986 and his doctoral thesis: "Finite Strip Method in Nonlinear Structural Problems" in 1988.

He worked at the "Traser" Design Bureau in Sarajevo as a designer and chief design engineer for bridges and tunnels (1978–1982). At the Faculty of Civil Engineering in Mostar, he worked as an assistant, assistant professor, and associate professor (1982–1992) and served as dean (1988–1992). At the Faculty of Technical Sciences in Novi Sad, he worked as an associate professor (1993–1996). He was appointed as a full professor at the Faculty of Civil Engineering in Subotica in 1998 and served as dean from 2006 to 2012. He has been working as a full professor at the Faculty of Architecture, Civil Engineering and Geodesy in Banja Luka since 1998. He was elected as a corresponding member of the Academy of Engineering Sciences of Serbia (AINS) in 2007 and as a full member in 2012.

He has participated in 61 national and international congresses, conferences, and symposia. He has published 29 papers in top international journals. He has supervised the completion of three doctoral dissertations and 63 final papers for bachelor's and master's degrees.

МЕМОРИЈСКЕ ОСОБИНЕ МАТЕРИЈАЛА

Сажетак: У раду се доказује да репрезентативна запремина стандарних цилиндричних узорака стијена, бетона и асфалта представља континуум из кога су узорци извађени или од кога ће конструкције бити изграђене. За доказ се користи реолошко-динамичка аналогија (РДА), стандардни експериментални подаци о узорцима и брзине П и С таласа добивене ултразвучним мјерењима. За разлику од свих до сада присутних теорија вишефазних материјала, РДА теорија у репрезентативној запремини јединствено описује чврсто стање и флуидан ток. Чврсто стање и флуидан ток су функционално повезани реолошким параметрима. Пластични коефицијенти смичуће вискозности описују (памте) материју у флуидном току у тренутку њеног природног настајања или вјештачког справљања.

Кључне ријечи: *реолошко динамичка аналогија, репрезентативна запремина, чврсто стање, флуидан ток, меморијске особине материјала*